Published online 17 November 2010 *Nucleic Acids Research, 2011, Vol. 39, No. 6* ***2045–2056***
doi:10.1093/nar/gkq875

Epigenetic control of a VDR-governed feed-forward loop that regulates p21$^{(waf1/cip1)}$ expression and function in non-malignant prostate cells

James L. Thorne[1], Orla Maguire[2], Craig L. Doig[2], Sebastiano Battaglia[2], Leah Fehr[3,4], Lara E. Sucheston[3,4], Merja Heinaniemi[5], Laura P. O'Neill[1], Christopher J. McCabe[1], Bryan M. Turner[1], Carsten Carlberg[5] and Moray J. Campbell[2,*]

[1]Institute of Biomedical Research, University of Birmingham, Edgbaston, B15 2TT, UK, [2]Department of Pharmacology and Therapeutics, [3]Department of Cancer Prevention and Control, Roswell Park Cancer Institute, Buffalo, NY 14263, [4]Department of Biostatistics, The State University of New York at Buffalo, Buffalo, NY 14214, USA and [5]Life Sciences Research Unit, Université du Luxembourg, 162A, Avenue de la Faïencerie, L-1511 Luxembourg, Luxembourg

Received July 1, 2010; Revised August 26, 2010; Accepted September 16, 2010

ABSTRACT

In non-malignant RWPE-1 prostate epithelial cells signaling by the nuclear receptor Vitamin D Receptor (VDR, NR1I1) induces cell cycle arrest through targets including *CDKN1A* (encodes p21$^{(waf1/cip1)}$). VDR dynamically induced individual histone modification patterns at three VDR binding sites (R1, 2, 3) on the *CDKN1A* promoter. The magnitude of these modifications was specific to each phase of the cell cycle. For example, H3K9ac enrichment occurred rapidly only at R2, whereas parallel accumulation of H3K27me3 occurred at R1; these events were significantly enriched in G_1 and S phase cells, respectively. The epigenetic events appeared to allow VDR actions to combine with p53 to enhance p21$^{(waf1/cip1)}$ activation further. In parallel, VDR binding to the *MCM7* gene induced H3K9ac enrichment associated with rapid mRNA up-regulation to generate miR-106b and consequently regulate p21$^{(waf1/cip1)}$ expression. We conclude that VDR binding site- and promoter-specific patterns of histone modifications combine with miRNA co-regulation to form a VDR-regulated feed-forward loop to control p21$^{(waf1/cip1)}$ expression and cell cycle arrest. Dissection of this feed-forward loop in a non-malignant prostate cell system illuminates mechanisms of sensitivity and therefore possible resistance in prostate and other VDR responsive cancers.

INTRODUCTION

Collectively, nuclear receptors (NRs) regulate a significant proportion of the human genome to exert diverse cellular function. Several NRs are attractive chemotherapy targets as the gene programs they control broadly inhibit cell proliferation and/or induce programmed cell death. For example, the anticancer actions of $1\alpha,25(OH)_2D_3$, the natural VDR (NR1I1) ligand, have been established for 30 years (1–3) and in certain cancer cell types including some prostate cancer cell lines (4–7), and xenograft and transgenic prostate cancer models (8,9). These effects are not universal and insensitivity is also apparent (10,11). In parallel, large-scale epidemiological studies found inverse associations between circulating levels of the pre-ligand, 25OH-D_3, and prostate cancer risk (12–20). However, despite these links between VDR signaling and broad anticancer activities, clinical exploitation in cancer has been slow.

Gene target expression by NRs has been intensively investigated from the perspective of receptor binding to response elements (21–24). These dynamics contribute to the patterns of target gene mRNA, however, the cycles vary considerably in timing and magnitude of response between different target genes and NRs. A complete

*To whom correspondence should be addressed. Tel: +7168453037; Fax: + 7168458857; Email: Moray.Campbell@RoswellPark.org
Present address:
James L. Thorne, Leeds Institute of Molecular Medicine, University of Leeds, Leeds LS9 7TF, UK.

The authors wish it to be known that, in their opinion, the first two authors should be regarded as joint First Authors.

understanding of the mechanisms that entrain these patterns and their biological significance remain elusive.

Against this backdrop, elucidating NR gene expression control mechanisms is important to illuminate mechanisms of resistance in cancer cells. In particular epigenetic resistance mechanisms have been explored. For example elevated levels of the NCOR2/SMRT co-repressor suppress VDR's ability to regulate a subset of target genes that mediate antiproliferative actions (25–27). In turn the accumulation of repressive histone modifications at suppressed target genes may allow for hypermethylation at adjacent CpG regions (28) and development of stable patterns of gene silencing [reviewed in refs. (29,30)].

MiRNA also contribute negative regulatory aspects to normal gene regulation, for example, as part of feed-forward loop motifs (31,32). Also NRs, including the VDR, are able to govern miRNA expression, and this in turn may contribute to resistance (33–37). The extent to which NR-regulated miRNA form feed-forward loops remains uncertain. Previously, we established that $1\alpha,25(OH)_2D_3$ regulates the DNA helicase *MCM7* (25) and others have established that miR-106b, located on intron 13 of the *MCM7* gene, inhibits the VDR target gene, *CDKN1A* (encodes $p21^{(waf1/cip1)}$) (38,39). Together these findings suggest that co-regulated miRNA may form an integral part of VDR signaling to control gene expression.

To investigate how VDR-regulated epigenetic events control target gene expression, we interrogated non-malignant RWPE-1 prostate epithelial cells (40) undergoing G_1 cell cycle arrest in response to $1\alpha,25(OH)_2D_3$ [reviewed in ref. (41)]. Specifically, we undertook a series of experiments to establish, if and to what extent VDR governed both histone modifications and miRNA expression to control gene expression. We focused on the circuitry that controls the *CDKN1A* gene and revealed that mRNA and protein modulation was determined by the spatial-temporal binding sequence of the VDR complex to two target genes; namely the *CDKN1A* gene itself and the *MCM-7* gene that gives rise to the miR-106b cluster. In this manner, $p21^{(waf1/cip1)}$ regulation arises due to the interplay of three processes: (i) gene- and response element-specific VDR-induced histone modifications, (ii) cell cycle status and (iii) co-regulation of miR-106b. These events generate a VDR feed-forward loop that regulates the magnitude, timing and sensitivity of $p21^{(waf1/cip1)}$ expression and hence cell cycle arrest. The regulation and function of this feed-forward loop provides insight into mechanisms of VDR sensitivity and resistance in prostate other VDR-responsive cancers.

MATERIALS AND METHODS

Agents, cell culture and antibodies

$1\alpha25(OH)_2D_3$ [gift of Dr Milan Uskokovic (BioXell S.p.A., Italy)] used at 100 nM concentration for all experiments. RWPE-1 non-malignant prostate epithelial cells and RWPE-2 cells were maintained in KSF media supplemented with EGF and BPE (Invitrogen, Paisley, UK). P69SV40T cells were cultured in RPMI with 10% FCS.

Antibodies for immunoblot: $p21^{(waf1/cip1)}$, beta-actin (Abcam, ab7960, ab8229). Antibodies for ChIP assays—VDR, NCOR1, RNA Pol II (Abcam ab3508, ab24552, ab26721), NCOR2/SMRT (Santa Cruz Biotechnologies sc1610), H3K27me3 (Upstate ABE44), H3K9ac, H3K9me2 and H3K4me3 [in house antibodies (42)]

Mice

Wild-type C57 BL/6xFVB mice were treated with EtOH or 20 μg/kg $1\alpha,25(OH)_2D_3$ for 12 or 24 h. Nine mice were used per treatment group. Prostate tissues pooled into three groups of three. RNA was isolated using TRIzol (Invitrogen).

Live cell sorting

Cells were stained with Hoechst 33342 (Invitrogen), which is a well-tolerated stain for DNA(43), fractionated using a MoFlo cell sorter (Beckman-Coulter, High Wycombe, UK) and Summit V4.3 software (Beckman-Coulter, UK) and 5×10^5 cells/phase were collected.

q-RT–PCR

RNA was isolated using TRizol (Invitrogen). Target gene expression was quantitated on an ABI 7900 [Applied Biosystems (http://www.appliedbiosystems.com)] machine. All primers and probes were as described previously (25). For miRNA quantitation, q-PCR was performed using Assay-on-Demand miR-106b and RNU48 probes. Measurements were performed in technical and biological triplicate.

Immunoblot analysis

Fifty microgram total protein extracts separated on 10% SDS gels, and blots probed with antibodies described above. Proteins detected using ECL (Amersham) and autoradiography.

ChIP protocols

X-ChIP was used to measure the association of VDR, NCOR1 and NCOR2/SMRT and RNA Pol II binding as described previously (44). Briefly, chromatin from 1.5×10^6 mid-exponential cells was cross-linked. Pre-cleared inputs were immunoprecipited with: VDR (Abcam ab3508), NCOR1 (Abcam ab24552), NCOR2/SMRT (Santa Cruz 1610), RNA Pol II (Abcam ab26721). Complexes were recovered using magnetic beads, washed, crosslinking reversed and further cleared DNA was recovered by standard precipitation approaches. Twenty-five nanogram DNA was used per Q-PCR reaction using SYBRgreen with pre-optimized primers (Table 1). To measure the interaction of VDR with co-repressors Re-ChIP was used. VDR immuno-complexes prepared with the VDR indicated in the X-ChIP section were eluted and immunoprecipitated with antibodies to NCOR1 or NCOR2/SMRT, new

Table 1. Primer sequences used for Q-PCR and ChIP analyses

Gene region	Forward	Reverse
Q-PCR		
MCM7	CGGTGCTGGTAGAAGGAGAG	AAACCCTGTACCACCTGTCG
MCM7 probe	GCCAATCCTGCGCACTGGGT	
X and N-ChIP		
MCM7, –7995	TACTTGGGAGGCTGAGATGG	CAGGCTGGAGTGCAGTGTTA
MCM7, –589	CCTAGCCCACCCAACCTTAT	TAATTCACAGTGCCCACAGG
CDKN1A, –7049 (R3)	AGCAGCACTGAAGCCTAACC	GAGAGGCCTACCAGCTTCAG
CDKN1A, –4496 (R2)	TAGAGATGCTCAGGCTGCTG	AGAGCTTCACCGACATAGCC
CDKN1A, –2137 (R1)	GAGGAAGGGGATGGTAGGAG	CTGGCAGATCACATACCCTGT
CDKN1A, TSS	TATATCAGGGCCGCGCTG	GGCTCCACAAGGAACTGACTTC
C-ChIP		
CDKN1A, TSS	CCGAAGTCAGTTCCTTGTGG	CGCTCTCTCACCTCCTCTGA
CDKN1A, –2137 (R1)	GCCTGTTTTCAGGTGAGGAA	CTGGCAGATCACATACCCTGT

immuno-complexes were formed and detection was as indicated for X-ChIP. N-ChIP was performed as previously described (45). Briefly, chromatin from 5×10^7 cells was harvested from nuclei and digested by micrococcal nuclease (Pharmacia, Milton Keynes, UK) and immunoprecipited with H3K27me3 (Upstate) (Abcam ab27472) or H3K9ac, H3K9me2 and H3K4me3 [in house antibodies (42)] or IgG control. DNA was purified and analyzed as for X-ChIP. C-ChIP was adapted from N-ChIP as previously described (46) by 'spiking' with SL2 cells prior to chromatin extraction and using human specific primers (Table 1).

MiR-106b knockdown

si-miR-106b (MI0000734, Dharmacon) and scrambled constructs (IN-001005-01-05, Dharmacon) transiently transfected into cells at 100 nM. Cells seeded into 6-well plates for treatment with EtOH or $1\alpha,25(OH)_2D_3$ (100 nM) and RNA isolated using TRizol (Invitrogen). For FACS analysis, cells were stained with Propidium Iodide solution, and run through a FACScan II (Becton Dickinson Biosciences). DNA histograms were analyzed using ModFit software (Verity Software House).

RESULTS

$1\alpha,25(OH)_2D_3$ induces cell cycle arrest associated with dynamic target gene regulation

$1\alpha,25(OH)_2D_3$ induced cell cycle arrest in RWPE-1 cells after 24 h exposure to ligand (Supplementary Figure S1). Co-incident with the cell cycle arrest, known VDR target genes (23,39,47,48) revealed significant $1\alpha,25(OH)_2D_3$-induced regulation, in bulk cell populations, compared to EtOH time-matched controls (Figure 1A). These patterns of mRNA accumulation were not readily predicted from the arrangement and location of vitamin D response elements (VDREs) in the promoter regions (23,39,47). These analyses suggested common and unique aspects of mRNA regulation. *CDKN1A, GADD45A* and *IGFBP3* displayed rapid modulation that returned to basal levels whereas *CYP24A1* displayed more sustained accumulation to a greater magnitude. *CYP24A1, GADD45A* and *CDKN1A* all displayed sequential repression, accumulation at 0.5 h, followed by repression. *IGFBP3* displayed no repression, but instead more immediate accumulation. Post 1 h, all genes displayed modulating accumulation with some degree of synchrony at 2 h that was generally reduced subsequently, although another peak was generally apparent at 12 h. $P21^{(waf1/cip1)}$ (encoded by *CDKN1A*) expression displayed distinct peaks at 1 and 3 h and a broader peak from 16 h onwards reflecting increased mRNA levels at 0.5, 2 and 12 h (Figure 1B). The dynamic regulation of *CDKN1A* over the first 1 h was also observed in the RAS-transformed variant of RWPE-1 cells, namely RWPE-2 (40) and in another prostate epithelial immortalized cell line, namely P69SV40T (49). These common VDR-regulated mRNA accumulation patterns in different prostate epithelial cell models suggest the mechanisms underlying this behavior are also common and shared (Supplementary Figure S2).

VDR-regulated histone modifications underpin CDKN1A regulation

Time-resolved quantitative ChIP approaches (0.5, 1, 4 and 12 h) at three VDRE regions (R1, R2, R3) (Figure 2A) (39). The spatial–temporal re-distribution of VDR and co-repressors was measured in parallel with regulation of a panel of histone modifications. Histone modifications measured were associated with either gene maintenance, namely H3K4me3 (the trithorax mark) and H3K27me3 (the polycomb mark), or others associated with dynamic regulation of transcription (H3K9ac and H3K9me2). These approaches revealed that $1\alpha,25(OH)_2D_3$ induced tightly regulated gene activating epigenetic events at only one response element on *CDKN1A*, namely R2 [from −4505 to −4489 from transcription start site (TSS)] (Figure 2B).

VDR accumulated rapidly at R2 after 0.5 and 1 h in response to $1\alpha,25(OH)_2D_3$ treatment and was associated with release of both co-repressors at 0.5 h (Figure 2B). N-ChIP approaches revealed parallel enrichment of H3K9ac and loss of repressive H3K9me2 at 0.5 h. At this time point, at the other response elements,

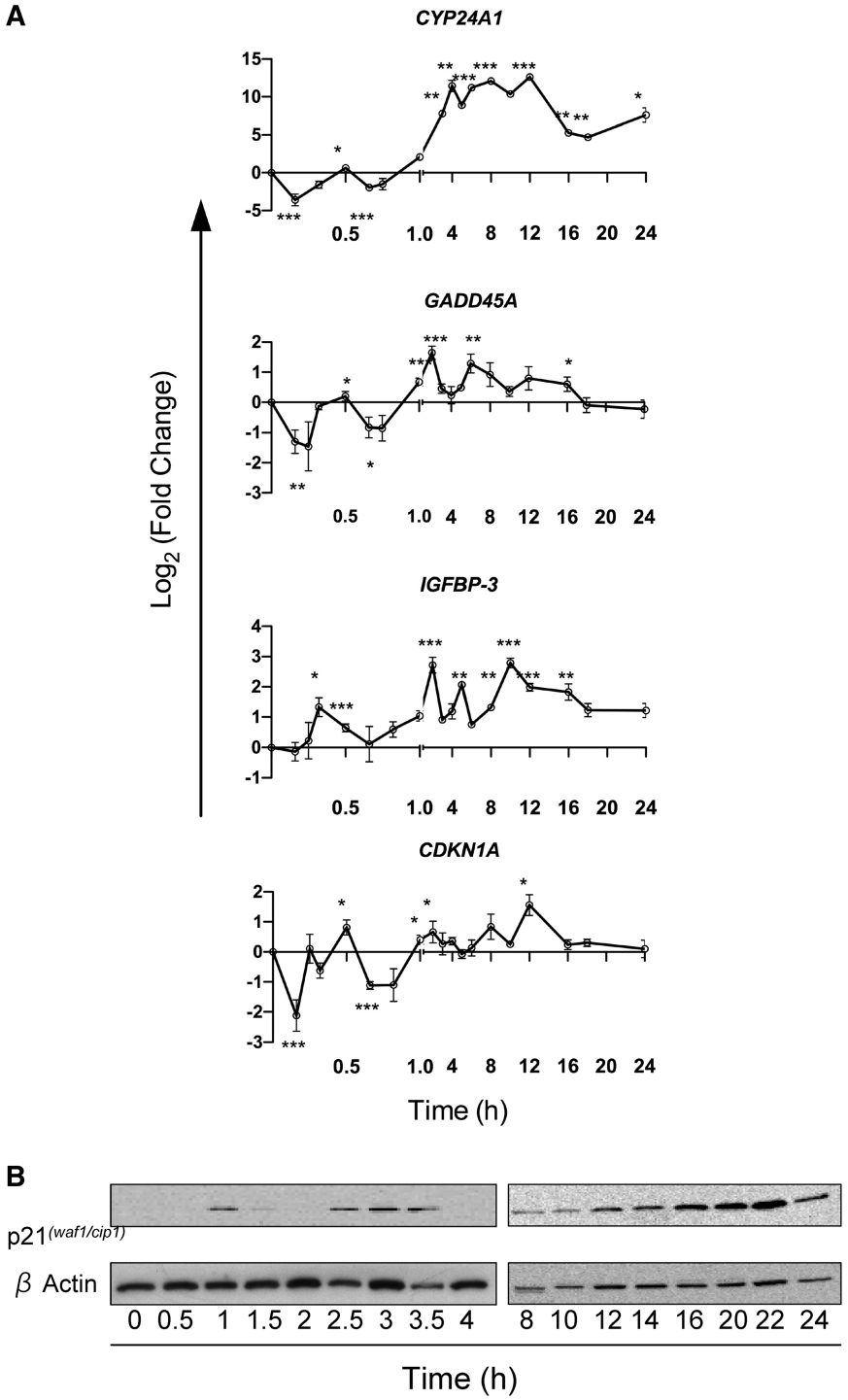

Figure 1. Dynamic regulation of VDR target genes. (**A**) RWPE-1 cells were treated with $1\alpha,25(OH)_2D_3$ (100 nM) or EtOH and mRNA was extracted at the indicated time points, and accumulation of indicated genes measured by TaqMan Q-RT–PCR. Accumulation of each target is given as $\log_2$ (fold change). Each data point represents the mean of triplicate experiments in triplicate wells ± SEM ($*P < 0.05$, $**P < 0.01$, $***P < 0.001$). All measurements performed in technical and biological triplicate. (**B**) Total cell proteins were isolated from cells treated as above at the indicated time points ($+D_3$) and subjected to western immunoblotting. Representative blots are shown for $p21^{(waf1/cip1)}$ (Abcam, ab7960). β-Actin used as a loading control (Abcam, ab8229). For quantification of signal Odyssey infrared imaging system (LI-COR, Lincoln, NE) was used and the quantification for the fold changes are under each image.

$1\alpha,25(OH)_2D_3$ actively induced association with co-repressor and/or enriched for repressive histone modifications. Thus significant enrichment of NCOR2/SMRT occurred at R3 (from −7059 to −7036) and of NCOR1 at R1 (from −2146 to −2129), the latter is associated with a loss of H3K9ac and enrichment of H3K9me2.

The activation state at R2 was rapid and reversed after 1 h. Thus following the initial accumulation at 0.5 h of an

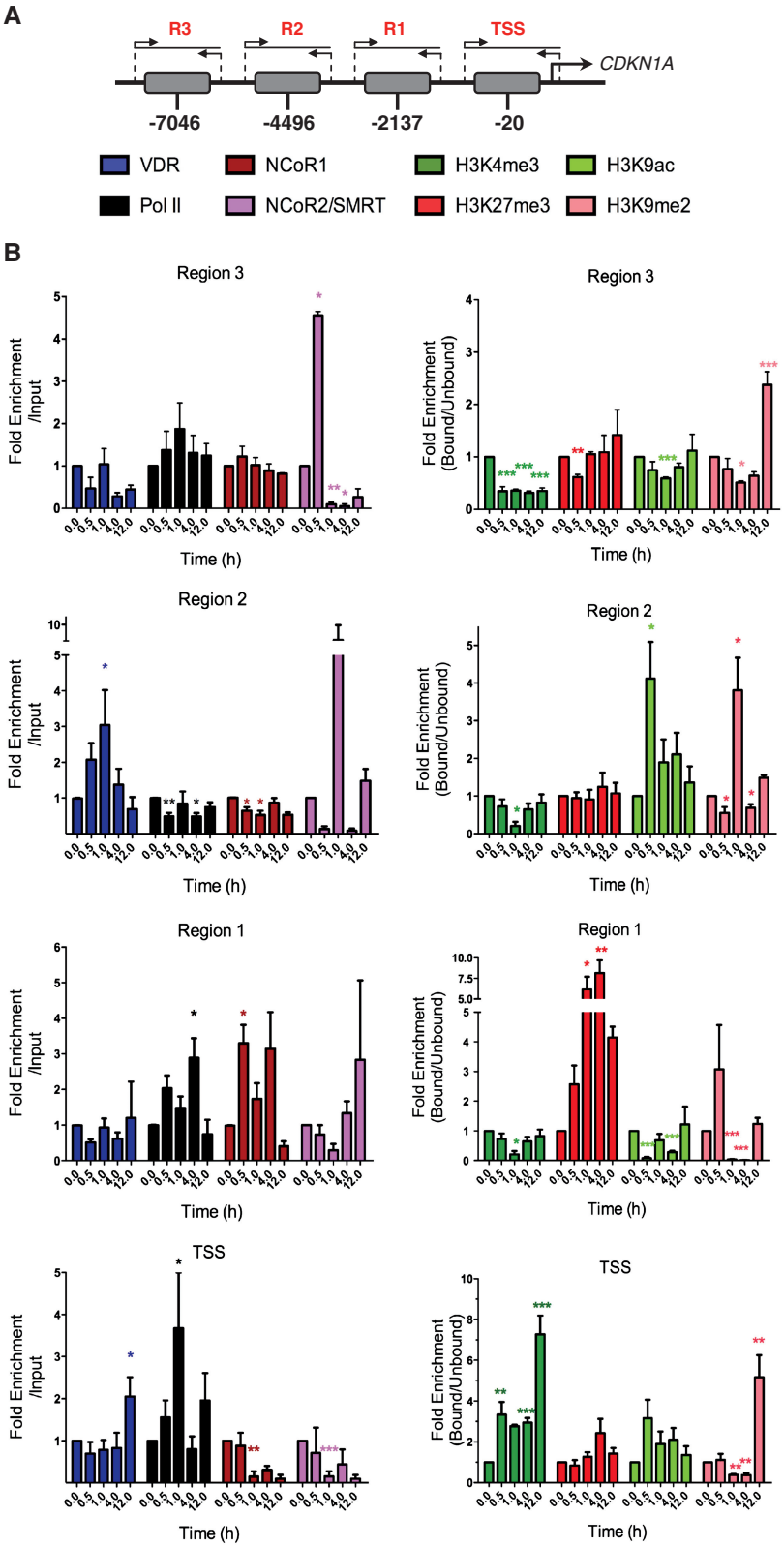

Figure 2. VDR-regulated epigenetic events on the promoter of *CDKN1A*. (**A**) The genomic location of the VDR binding regions (R3, R2 and R1) on *CDKN1A* and the transcription start site (TSS). (**B**) *Left graphs*. RWPE-1 bulk populations treated with 1α,25$(OH)_2D_3$ (100 nM) or EtOH for indicated time points. Association of RNA Pol II, VDR, NCOR1 and NCOR2/SMRT was measured at each region by X-ChIP using ChIP grade antibodies and normalized and given as fold enrichment over input as described previously (44). Primers are shown in Table 1. Enrichment was measured by Q-PCR with primers specific to these regions that amplified a product <150 bp. *Right graphs*. Parallel changes to histone modifications (H3K9me2, H3K27me3, H3K4me3 and H3K9ac) were assayed using N-ChIP and normalized using bound over unbound DNA pulled down with specific ChIP grade antibodies (42). N-ChIP was performed as previously described (53). Enrichment was measured by Q-PCR as above. All measurements performed in technical duplicate and biological triplicate.

'active' receptor and epigenetic signature (Figure 2B) and mRNA and protein accumulation (Figure 1), NCOR2/SMRT and H3K9me2 were re-enriched for 1 h at R2, with loss of H3K9ac levels, underscoring the tight control of these activation events. In contrast, the repressive events at R3 and R1 were more sustained, notably at R1 where H3K27me3 accumulated from 1 h onwards through to 12 h (Figure 2B). It is also interesting to note that NCOR/SMRT enrichment appears to move along the promoter from R3 (0.5 h) to R2 (1 h) to R1 (12 h) also suggesting longer term effects on the promoter. The TSS also displayed sustained H3K4me3 enrichment after 0.5 h as NCOR1 and NCOR2/SMRT levels declined. H3K4me3 enrichment continued to 12 h, as did RNA Pol II and accompanied mRNA and protein accumulation at 12 h.

Re-ChIP analyses were undertaken at R2 and R1 as these regions reflected the parallel but distinct activation and repression observed upon $1\alpha,25(OH)_2D_3$ treatment. These analyses under scored the role of co-repressor release and recapture. NCOR1 interactions with VDR were significantly reduced at both regions after 0.5 h although this was only co-incident with H3K9ac gain at R2 (Figure 3A). Subsequently, NCOR1 significantly re-associated with VDR, most noticeably at R2, at 1 h onwards, co-incident with increased H3K9me2 in this region (Figure 2). NCOR2/SMRT did not dissociate from the VDR, but rather trended to accumulation at 4 h at R2 and reflected the co-repressor enrichment in this region at this time point (Figure 2).

At certain time points the *CDKN1A* locus displayed both activating and repressing histone modifications, whereas mRNA expression was at basal levels. For example, after 1 h the TSS and body of the gene displayed enrichment for H3K9ac and H3K4me3 (Figure 2 and data not shown), whereas regions R2 and R1 were enriched for H3K9me2 and H3K27me3, respectively. We investigated whether this represented a so-called poised state and whether the *CDKN1A* locus could be activated by further transcriptional activators. Regions R1 and R2 are within close proximity to p53 binding sites (39,50). We therefore tested if the p53 activator 5-flurouracil enhanced $1\alpha,25(OH)_2D_3$-induced *CDKN1A* mRNA accumulation over a 4 h time course and revealed significantly co-operative actions at 1 h (Figure 3B). The combination of agents yielded a significant combined effect at 1 h; comparable events were observed with *IGFBP3*, another target regulated by VDR and p53 (Figure 3B) (51).

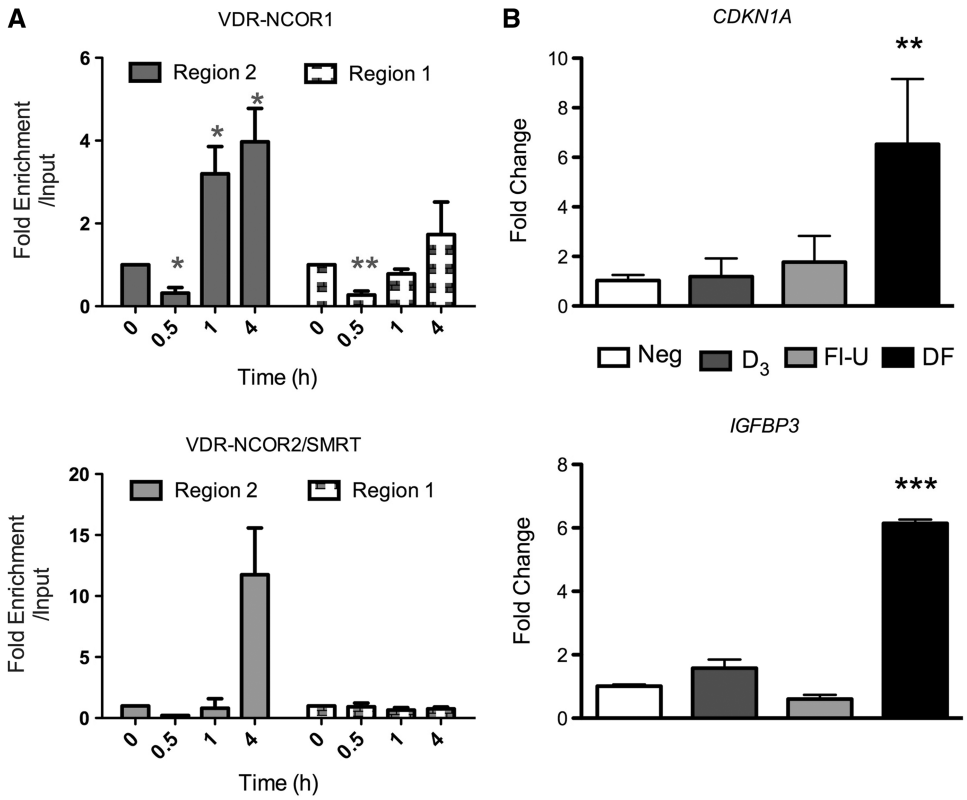

Figure 3. VDR interactions with co-repressors and the enhancement of $1\alpha,25(OH)_2D_3$-induced target gene expression. (**A**) RWPE-1 cells were treated as above, and X-ChIP performed and VDR DNA–protein complexes were eluted and immunoprecipitated with antibodies to NCOR1 or NCOR2/SMRT. Enrichment was measured by Q-PCR with primers specific to these regions that amplified a product less than 150 bp. Primers are shown in Table 1. All measurements performed in technical duplicate and biological triplicate. (**B**) RWPE-1 cells were treated with $1\alpha,25(OH)_2D_3$ (100 nM), 5-flurouracil (Fl-U) (50 nM), or combination (DF) for 1 h. Accumulation of *CDKN1A* and *IGFBP3* measured by TaqMan Q-PCR. All measurements performed in technical and biological triplicate ($*P < 0.05$, $**P < 0.01$, $***P < 0.001$).

Cell cycle status determines the magnitude of histone modifications on the CDKN1A promoter

Previous Q-PCR approaches in FACS-sorted RWPE-1 cells revealed S-phase elevation of co-repressors (for example *NCOR1*, *NCOR2/SMRT*) and HDACs (for example *HDACs 2* and *3*), whereas *VDR* and was broadly equivalent through the cell cycle [(52) and data not shown]. We therefore reasoned that the mixture of activating and repressing histone modifications may represent cells in different cell cycle states, for example, that S-phase cells would not be epigenetically responsive to VDR activation. To address this possibility, we FACS-sorted cells into different phases of the cell cycle and examined VDR-induced changes in histone modifications through the cell cycle using Carrier-ChIP (C-ChIP) approaches (53) (Figure 4).

Again, focusing on two response regions that displayed distinct activation events at 0.5 h, we revealed that after 0.5 h, $1\alpha,25(OH)_2D_3$ induced significant H3K27me3 enrichment at R1 in S and G_2/M phase cells only (Figure 4A). At the basal level there were two pronounced differences in G_1 cells compared to the other phases, with H3K9ac enrichment at R1 at the TSS (data not shown). Interestingly in bulk culture upon treatment with $1\alpha,25(OH)_2D_3$ H3K27me3 levels trended to enrichment after 0.5 h, however it was not significant, but this became significant when considering the individual phases of the cell cycle. Similar phase-specific patterns of H3K9ac enrichment occurred in G1 cells only at the TSS, and again this was not significant when considering bulk population cells but was when considering G_1 phase cells only (Figure 4B).

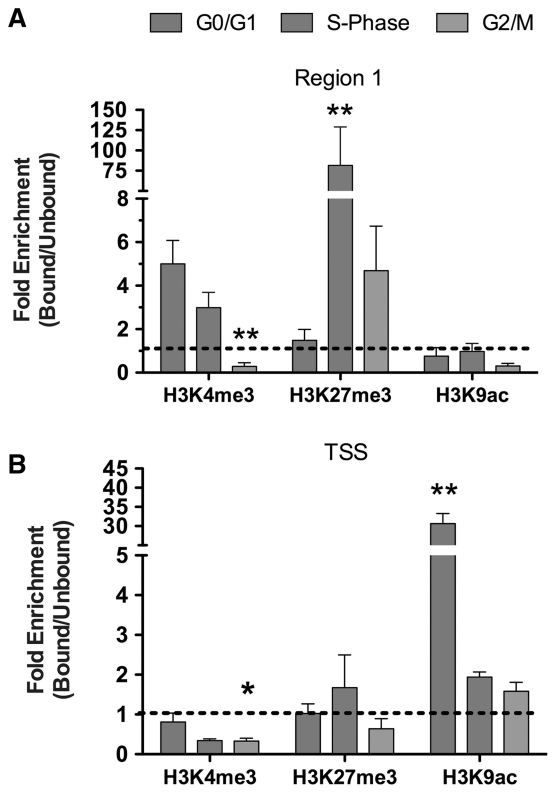

Figure 4. The cell cycle determines the magnitude of VDR-regulated histone modification. RWPE-1 cells were treated with $1\alpha,25(OH)_2D_3$ (100 nM) for 0.5 h prior to being FACS-sorted into the different phases of the cell cycle. Cells stained with Hoechst 33342 (Invitrogen), fractionated using a MoFlo cell sorter (Beckman-Coulter, High Wycombe, UK) and Summit V4.3 software (Beckman-Coulter, UK) and 5×10^5 cells/phase collected. Induced changes to repressive (H3K27me3) and activating (H3K4me3 and H3K9ac) histone modifications at R1 and the TSS on the *CDKN1A* promoter were interrogated using Carrier-ChIP protocols, C-ChIP was adapted from N-ChIP as previously described (46) by 'spiking' with SL2 cells prior to chromatin extraction and using human specific primers (Table 1). Histone modifications were assayed using N-ChIP and normalized using bound over unbound DNA pulled down with specific antibodies. Each data point represents the mean of triplicate experiments in duplicate wells ± S.E.M. (*$P < 0.05$, **$P < 0.01$).

Co-regulation of miR-106b is critical to regulate $p21^{(waf1/cip1)}$ expression

$1\alpha,25(OH)_2D_3$ treatment up-regulated *MCM7*, and consequently miR-106b, in a highly similar manner to *CDKN1A*. That is, *MCM7* accumulated at 0.25 h, miR-106b at 0.33 h, prior to the initial *CDKN1A* expression at 0.5 h (Figure 5A). Two VDR binding regions on the *MCM7* promoter were identified *in silico* and demonstrated the same rate of VDR binding over the first 0.5 h compared to R2 of *CDKN1A* (Figure 5B). We also examined the enrichment of the same four histone modifications as measured at the *CDKN1A* promoter and found that only H3K9ac was clearly enriched at −7995 (0.5 h) and the TSS (1 h) (Figure 5C). In contrast the repressive histone modifications (H3K9me2 and H3K27me3) were not significantly altered at either the two VDR binding regions or the TSS. These data suggest that *MCM7* has an intrinsically more responsive promoter. However, the rate is similar of VDR binding kinetics to the critical activating response elements, either R2 of the *CDKN1A* gene or at position −7995 of the *MCM7* gene. Therefore the receptor binding kinetics alone do not explain the altered mRNA accumulation rate between the genes *CDKN1A* and *MCM7* (Figure 5A).

Therefore, we investigated the contribution of miR-106b to control $p21^{(waf1/cip1)}$ expression and cell cycle arrest. Firstly intervention with miRNA knockdown approaches resulted in ~50% knockdown and caused $1\alpha,25(OH)_2D_3$ treatment to induce *CDKN1A* accumulation to the same extent, but at a significantly earlier time point (Figures 1A, 5A and D) thus suggesting a role to control mRNA accumulation rates. In parallel, we established that the same miRNA knockdown approaches allowed $p21^{(waf1/cip1)}$ to be induced to a higher level (Figure 5E) leading to an enhanced $1\alpha,25(OH)_2D_3$ driven G_1 arrest (Figure 5F). These data suggest that miR-106b also plays a role in governing translation rates, as the area under the curve of mRNA accumulation did not differ significantly with miR-106b siRNA (Figure 5D). Interestingly at later time points (22 h) miR-106b also accumulated and appears to correlate with the loss of $p21^{(waf1/cip1)}$ expression after 22 h (Figure 1B and Supplementary Figure S3). Finally, the relationship between *Cdkn1a* and miR-106b appears

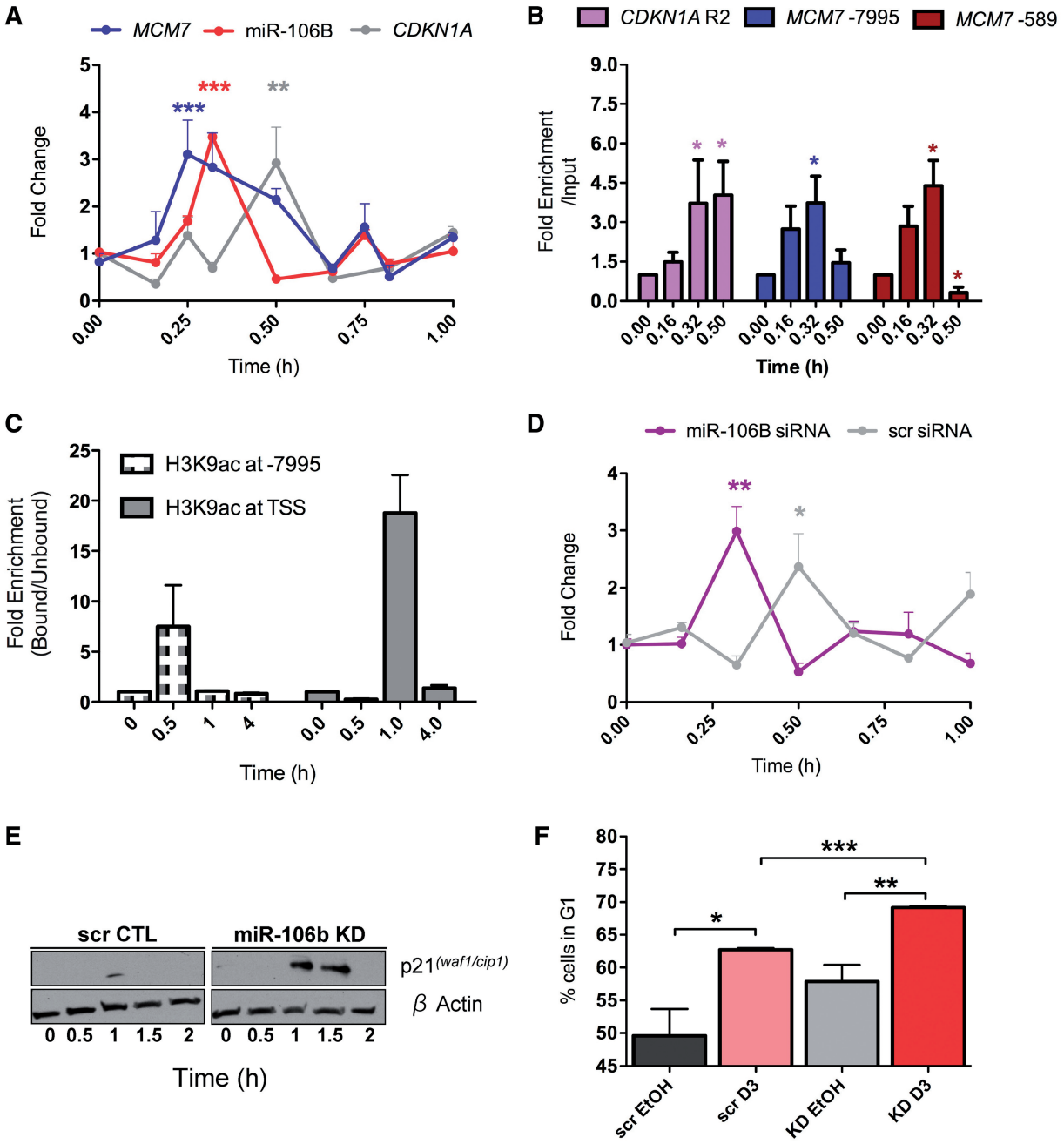

Figure 5. MiR-106b co-expression governs p21$^{(waf1/cip1)}$ expression and cell cycle arrest. (**A**) RWPE-1 cells were treated with 1α,25(OH)$_2$D$_3$ (100 nM) or EtOH control for indicated time points, mRNA extracted, and levels of accumulation of indicated genes measured by TaqMan Q-PCR. For miRNA quantitation, Q-PCR performed using Assay-on-Demand miR-106b and RNU48 probes. All measurements performed in technical and biological triplicate. (**B**) Cells were treated as in A, chromatin extracted and VDR binding to the indicated VDREs in the *MCM7* promoter, and R2 on the *CDKN1A* promoter was measured, as indicated in Figure 2. (**C**) Changes to H3K9ac were assayed using N-ChIP and normalized using bound over unbound DNA pulled down with specific ChIP grade antibodies (42). N-ChIP was performed as previously described (53). Enrichment was measured by Q-PCR as above. All measurements performed in technical and biological triplicate. (**D**) 100nM si-miR-106b (MI0000734, Dharmacon) and scrambled constructs (IN-001005-01-05, Dharmacon) transiently transfected into cells. Following transfection, cells were treated as above. *CDKN1A* mRNA expression was measured by TaqMan Q-PCR as in Figure 1A. All data points on panels A and D represent the mean of triplicate experiments amplified in triplicate wells ± SEM (*$P < 0.05$, **$P < 0.01$, ***$P < 0.005$). (**E**) The effect of mir-106b knockdown on p21$^{(waf1/cip1)}$ expression. Cells were treated as in panel C and p21$^{(waf1/cip1)}$ detected by western blot as in Figure 1B, and both scr and siRNA blots exposed for 30 s. (**F**) The effect of 1α,25(OH)$_2$D$_3$ treatment on cell cycle arrest was measured in the indicated treatment groups. For FACS analysis, cells were stained with Propidium Iodide solution and run through a FACScan II (Becton Dickinson Biosciences). DNA histograms were analyzed using ModFit software (Verity Software House). Results were plotted as percent of cells seen in G$_1$ phase and each data point represents the mean of three separate experiments ± SEM (*$P < 0.05$, **$P < 0.01$, ***$P < 0.005$).

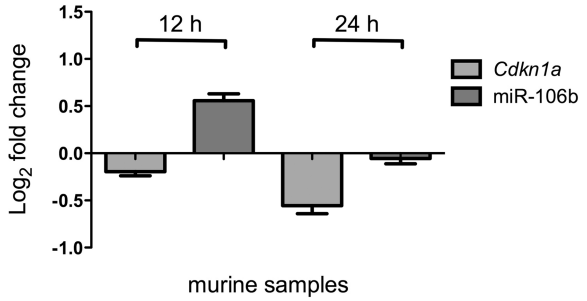

Figure 6. *In vivo* regulation of *Cdkn1a* and miR-106b in murine prostate. C57 BL/6xFVB WT mice were treated with $1\alpha,25(OH)_2D_3$ (20 μg/kg) or equal volume of EtOH for 12 or 24 h. Mice ($n = 9$) in each control and treatment group were sacrificed and the prostate removed and pooled into three groups of three, mRNA extracted using TRIzol (Invitrogen), and *Cdkn1a* and miR-106b levels were measured by TaqMan Q-PCR. Accumulation of each target is given as $\log_2$ (fold change). Each data point represents the mean ± SEM. A significant induction of miR-106b was observed at 12 h, and at 12 and 24 h *Cdkn1a* was significantly repressed. (**$P < 0.01$).

detectable in the prostates of normal C57 BL/6xFVB mice at 12 and 24 h post-treatment with $1\alpha25(OH)_2D_3$ (20 μg/kg). Notably at 12 h there was a significant increase in miR-106b and corresponding repression of *Cdkn1a* (Figure 6).

DISCUSSION

Transcriptional kinetics, even for the same NRs, are highly variable depending upon the cell type and target gene. These ambiguities are compounded by the frequent use of cancer cell lines to study these kinetics. Problematically, these cells frequently contain corruptions to the very mechanisms being studied, including elevated NCOR1 and NCOR2/SMRT expression (25,26,54,55). This is apparent when considering the VDR where, in malignant systems, $1\alpha,25(OH)_2D_3$ induced *CDKN1A* accumulation appears highly variable, often being either significantly delayed or absent despite apparently adequate receptor expression (44,56,57). Analogous studies on the estrogen receptor α revealed rapid binding to target genes, occurring in the order of minutes, but is non-functional as it results in neither mRNA nor protein expression changes (22,58). In contrast, other NRs, interrogated with different technologies, have suggested highly rapid cycling (59).

The current study informs these debates by utilizing an endogenous promoter, in a non-malignant cell system, where the response to ligand approximates closely to a normal response. Rapid and dynamic patterns of mRNA accumulation occurred for four VDR target genes, and there was a degree of response synchrony especially in early events. We established for one target, *CDKN1A*, that the patterns of mRNA accumulation reflected receptor and co-repressor exchanges occurring in a unique manner at each of three VDREs. In turn, these events drove unique patterns of histone modifications. Activation events occurred at only one response element (R2) after 0.5 h and were reflected by increased mRNA accumulation and protein expression. It is tempting to speculate that the immediate repressive events occurring at R3 and R1 contribute to the reduced mRNA levels for *CDKN1A* that occur at earlier time points. Collectively, these results support the concept that in non-malignant systems NR transcriptional responses can be rapid and functional, and faithfully lead to changes in protein. The transition through activated epigenetic states appears to allow the integration of transcriptional signals, for example through co-operation with p53 at 1 h and suggests an epigenetic basis for the observed co-operation between these two pathways (39,60–63). The co-operative effects at 1 h also support the p53 functional status of RWPE-1 cells and reflects the fact human papillomavirus 18 (HPV 18) immortalized cells do not necessarily target p53 (40).

We undertook univariate linear regression analyses to identify patterns of associations within these data sets. These approaches identified the most significant association occurred after 4 h, where the locus appeared to return to a resting state, characterized by a significant association at between VDR, NCOR1 and H3K27me3 ($P < 0.05$) at the TSS and R1 (data not shown). These findings support an emerging view of this histone mark being more dynamically regulated than previously appreciated (64,65) and suggest its regulation is part of sequential epigenetic steps in the control of transcription. These data suggest that the regulation of H3K27me3 at specific response elements act as a marker of the return to the basal state and forms part of a biological ratchet to regulate dynamic transcriptional patterns (66).

We made the further discoveries that the magnitude of epigenetic modulation was refined by the cell cycle status. ChIP approaches in FACS-sorted cells revealed that G_1 phase cells were characterized by enhanced VDR-induced activating histone modifications (for example H3K9ac), with S and G_2/M phases being largely repressive, for example, with H3K27me3 enrichment at region R1. Thus events, which were not significant when considering bulk populations, emerged with significant clarity when considering each specific cell cycle phase and underscore the fact that bulk culture findings represent an average event of potentially very different populations. While other NRs have been demonstrated to display cell cycle-specific phases of activation (67,68), the current study supports an underlying role for differential regulation of histone modifications through the cell cycle to govern these actions. Together these data suggest the magnitude of the *CDKN1A* activation, at least at early time points, is influenced significantly by the stage of the cell cycle.

We added further to this understanding by establishing VDR-dependent co-regulation of miR-106b to modulate the precise timing of *CDKN1A* accumulation and also the expression of $p21^{(waf1/cip1)}$, and consequential cell cycle arrest. Together these data demonstrate that VDR induced regulation of $p21^{(waf1/cip1)}$ is determined by interplay of histone modifications and miRNA expression that combine in a feed-forward loop. Key regulatory aspects of this loop are the re-distribution of VDR binding and co-repressor associations to govern histone modifications of two gene targets and the status of the cell cycle. The cell

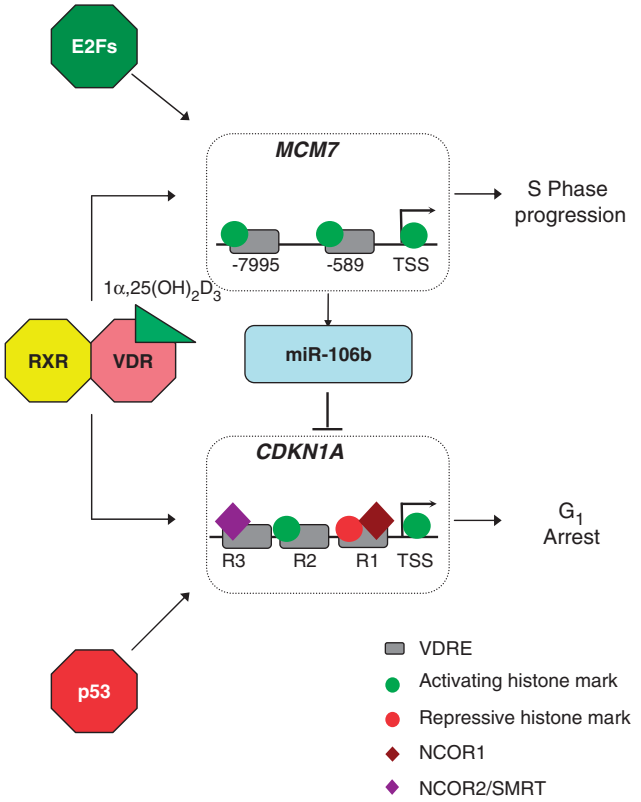

Figure 7. A proposed VDR governed feed-forward loop to control p21$^{(waf1/cip1)}$. The VDR complex binds to both the *CDKN1A* gene [encodes p21$^{(waf1/cip1)}$] and the DNA helicase gene *MCM7*. Over the first hour of activation only one response element on *CDKN1A* responds in a positive manner with loss of co-repressors and increased H3K9ac levels. The other response elements display repressive events. In parallel increased H3K9ac enrichment is observed at all response elements and the TSS of the *MCM7* gene. The mixture of regulated epigenetic events on the *CDKN1A* promoter is significantly influenced by the status of the cell cycle and allows for cross-talk with p53, which also targets *CDKN1A* directly (response elements not shown) to sustain cell cycle arrest. The *MCM7* gene is a target of S-phase transcription factors such as E2F family members and therefore this feed-forward loop fine tunes p21$^{(waf1/cip1)}$ expression in the context of cell cycle progression.

cycle component appears to open windows with which other activators may exert an effect, for example p53, to modulate the magnitude of effects. Given that the *MCM7* gene is a key target of S-phase transcription factors such as the E2F family members, this loop represents a balance between transcription factors that promote either G_1 arrest or S-phase progression (summarized in Figure 7). Given that NR biology appears illustrative of basic mechanisms of transcription factor control the current findings may apply generally to gene regulatory mechanisms.

The expression of miRNA contained within feed-forward motifs is disrupted in cancer (69,70). For example, the cellular advantage to retaining the *MCM-7* promoter selectively in an active state (25) has recently been underscored in prostate cancer by establishing that miR-106b is a proto-oncogene (71). A strong emerging literature now supports the concept that tumors changes in miRNA regulation is translated to altered serum expression and therefore offers an important diagnostic and prognostic therapeutic window (72–75). In this manner, the regulation of miRNA such as miR-106b in feed-forward loop motifs may be critical biomarkers to monitor VDR responsiveness. The current studies open up the door to the possibility that serum expression of VDR tumor-regulated miRNA define molecular phenotypes associated with prostate cancer aggressiveness and responsiveness to vitamin D compound treatment.

SUPPLEMENTARY DATA

Supplementary Data are available at NAR Online.

ACKNOWLEDGEMENTS

$1\alpha25(OH)_2D_3$ was a gift from Dr Milan Uskokovic (BioXell S.p.A., Italy).

FUNDING

Funding for open access charge: M.J.C. acknowledges the support of *NucSys*, a European Community FP6-Marie Curie Research Training Network, the Biotechnology and Biological Sciences Research Council, and in part, support from National Institute of Health grants RO1 CA095367-06 and 2R01-CA-095045-06, and the NCI Cancer Center Support Grant to the Roswell Park Cancer Institute [CA016056]. B.M.T. is supported by program grant C1015/A9077 from Cancer Research UK.

Conflict of interest statement. None declared.

REFERENCES

1. Colston,K., Colston,M.J. and Feldman,D. (1981) 1,25-dihydroxyvitamin D3 and malignant melanoma: the presence of receptors and inhibition of cell growth in culture. *Endocrinology*, **108**, 1083–1086.
2. Miyaura,C., Abe,E., Kuribayashi,T., Tanaka,H., Konno,K., Nishii,Y. and Suda,T. (1981) 1 alpha,25-Dihydroxyvitamin D3 induces differentiation of human myeloid leukemia cells. *Biochem. Biophys. Res. Commun.*, **102**, 937–943.
3. Abe,E., Miyaura,C., Sakagami,H., Takeda,M., Konno,K., Yamazaki,T., Yoshiki,S. and Suda,T. (1981) Differentiation of mouse myeloid leukemia cells induced by 1 alpha,25-dihydroxyvitamin D3. *Proc. Natl Acad. Sci. USA*, **78**, 4990–4994.
4. Campbell,M.J., Elstner,E., Holden,S., Uskokovic,M. and Koeffler,H.P. (1997) Inhibition of proliferation of prostate cancer cells by a 19-nor-hexafluoride vitamin D3 analogue involves the induction of p21waf1, p27kip1 and E-cadherin. *J. Mol. Endocrinol.*, **19**, 15–27.
5. Elstner,E., Campbell,M.J., Munker,R., Shintaku,P., Binderup,L., Heber,D., Said,J. and Koeffler,H.P. (1999) Novel 20-epi-vitamin D3 analog combined with 9-cis-retinoic acid markedly inhibits colony growth of prostate cancer cells. *Prostate*, **40**, 141–149.
6. Peehl,D.M., Skowronski,R.J., Leung,G.K., Wong,S.T., Stamey,T.A. and Feldman,D. (1994) Antiproliferative effects of 1,25-dihydroxyvitamin D3 on primary cultures of human prostatic cells. *Cancer Res.*, **54**, 805–810.
7. Colston,K., Colston,M.J., Fieldsteel,A.H. and Feldman,D. (1982) 1,25-dihydroxyvitamin D3 receptors in human epithelial cancer cell lines. *Cancer Res.*, **42**, 856–859.
8. Blutt,S.E., Polek,T.C., Stewart,L.V., Kattan,M.W. and Weigel,N.L. (2000) A calcitriol analogue, EB1089, inhibits the

growth of LNCaP tumors in nude mice. *Cancer Res.*, **60**, 779–782.
9. Banach-Petrosky,W., Ouyang,X., Gao,H., Nader,K., Ji,Y., Suh,N., DiPaola,R.S. and Abate-Shen,C. (2006) Vitamin D inhibits the formation of prostatic intraepithelial neoplasia in Nkx3.1;Pten mutant mice. *Clin. Cancer Res.*, **12**, 5895–5901.
10. Campbell,M.J., Gombart,A.F., Kwok,S.H., Park,S. and Koeffler,H.P. (2000) The anti-proliferative effects of 1alpha,25(OH)2D3 on breast and prostate cancer cells are associated with induction of BRCA1 gene expression. *Oncogene*, **19**, 5091–5097.
11. Rashid,S.F., Moore,J.S., Walker,E., Driver,P.M., Engel,J., Edwards,C.E., Brown,G., Uskokovic,M.R. and Campbell,M.J. (2001) Synergistic growth inhibition of prostate cancer cells by 1 alpha,25 Dihydroxyvitamin D(3) and its 19-nor-hexafluoride analogs in combination with either sodium butyrate or trichostatin A. *Oncogene*, **20**, 1860–1872.
12. Garland,C.F. and Garland,F.C. (1980) Do sunlight and vitamin D reduce the likelihood of colon cancer? *Int. J. Epidemiol.*, **9**, 227–231.
13. Garland,F.C., Garland,C.F., Gorham,E.D. and Young,J.F. (1990) Geographic variation in breast cancer mortality in the United States: a hypothesis involving exposure to solar radiation. *Prev. Med.*, **19**, 614–622.
14. Luscombe,C.J., French,M.E., Liu,S., Saxby,M.F., Jones,P.W., Fryer,A.A. and Strange,R.C. (2001) Prostate cancer risk: associations with ultraviolet radiation, tyrosinase and melanocortin-1 receptor genotypes. *Br. J. Cancer*, **85**, 1504–1509.
15. Giovannucci,E. (2005) The epidemiology of vitamin D and cancer incidence and mortality: a review (United States). *Cancer Causes Control*, **16**, 83–95.
16. Schwartz,G.G. and Hulka,B.S. (1990) Is vitamin D deficiency a risk factor for prostate cancer? (Hypothesis). *Anticancer Res.*, **10**, 1307–1311.
17. John,E.M., Schwartz,G.G., Koo,J., Van Den,B.D. and Ingles,S.A. (2005) Sun exposure, vitamin D receptor gene polymorphisms, and risk of advanced prostate cancer. *Cancer Res.*, **65**, 5470–5479.
18. Chen,T.C., Wang,L., Whitlatch,L.W., Flanagan,J.N. and Holick,M.F. (2003) Prostatic 25-hydroxyvitamin D-1alpha-hydroxylase and its implication in prostate cancer. *J. Cell Biochem.*, **88**, 315–322.
19. Hsu,J.Y., Feldman,D., McNeal,J.E. and Peehl,D.M. (2001) Reduced 1alpha-hydroxylase activity in human prostate cancer cells correlates with decreased susceptibility to 25-hydroxyvitamin D3-induced growth inhibition. *Cancer Res.*, **61**, 2852–2856.
20. Ahonen,M.H., Tenkanen,L., Teppo,L., Hakama,M. and Tuohimaa,P. (2000) Prostate cancer risk and prediagnostic serum 25-hydroxyvitamin D levels (Finland). *Cancer Causes Control*, **11**, 847–852.
21. Rosenfeld,M.G., Lunyak,V.V. and Glass,C.K. (2006) Sensors and signals: a coactivator/corepressor/epigenetic code for integrating signal-dependent programs of transcriptional response. *Genes Dev.*, **20**, 1405–1428.
22. Metivier,R., Penot,G., Hubner,M.R., Reid,G., Brand,H., Kos,M. and Gannon,F. (2003) Estrogen receptor-alpha directs ordered, cyclical, and combinatorial recruitment of cofactors on a natural target promoter. *Cell*, **115**, 751–763.
23. Vaisanen,S., Dunlop,T.W., Sinkkonen,L., Frank,C. and Carlberg,C. (2005) Spatio-temporal activation of chromatin on the human CYP24 gene promoter in the presence of 1alpha,25-dihydroxyvitamin D(3). *J. Mol. Biol.*, **350**, 65–77.
24. Kang,Z., Janne,O.A. and Palvimo,J.J. (2004) Coregulator recruitment and histone modifications in transcriptional regulation by the androgen receptor. *Mol. Endocrinol.*, **18**, 2633–2648.
25. Khanim,F.L., Gommersall,L.M., Wood,V.H., Smith,K.L., Montalvo,L., O'Neill,L.P., Xu,Y., Peehl,D.M., Stewart,P.M., Turner,B.M. *et al.* (2004) Altered SMRT levels disrupt vitamin D3 receptor signalling in prostate cancer cells. *Oncogene*, **23**, 6712–6725.
26. Kim,J.Y., Son,Y.L. and Lee,Y.C. (2008) Involvement of SMRT corepressor in transcriptional repression by the vitamin D receptor. *Mol. Endocrinol*, **23**, 251–264.
27. Ting,H.J., Bao,B.Y., Reeder,J.E., Messing,E.M. and Lee,Y.F. (2007) Increased expression of corepressors in aggressive androgen-independent prostate cancer cells results in loss of 1alpha,25-dihydroxyvitamin D3 responsiveness. *Mol. Cancer Res.*, **5**, 967–980.
28. Yoon,H.G., Chan,D.W., Reynolds,A.B., Qin,J. and Wong,J. (2003) N-CoR mediates DNA methylation-dependent repression through a methyl CpG binding protein Kaiso. *Mol. Cell*, **12**, 723–734.
29. Battaglia,S., Maguire,O. and Campbell,M.J. (2010) Transcription factor co-repressors in cancer biology; roles and targeting. *Int. J. Cancer*, **126**, 2511–2519.
30. Mohn,F. and Schubeler,D. (2009) Genetics and epigenetics: stability and plasticity during cellular differentiation. *Trends Genet.*, **25**, 129–136.
31. Mangan,S. and Alon,U. (2003) Structure and function of the feed-forward loop network motif. *Proc. Natl Acad. Sci. USA*, **100**, 11980–11985.
32. Mangan,S., Itzkovitz,S., Zaslaver,A. and Alon,U. (2006) The incoherent feed-forward loop accelerates the response-time of the gal system of Escherichia coli. *J. Mol. Biol.*, **356**, 1073–1081.
33. Gatfield,D., Le Martelot,G., Vejnar,C.E., Gerlach,D., Schaad,O., Fleury-Olela,F., Ruskeepaa,A.L., Oresic,M., Esau,C.C., Zdobnov,E.M. *et al.* (2009) Integration of microRNA miR-122 in hepatic circadian gene expression. *Genes Dev.*, **23**, 1313–1326.
34. Song,G. and Wang,L. (2008) Transcriptional mechanism for the paired miR-433 and miR-127 genes by nuclear receptors SHP and ERRgamma. *Nucleic Acids Res.*, **36**, 5727–5735.
35. Ribas,J., Ni,X., Haffner,M., Wentzel,E.A., Salmasi,A.H., Chowdhury,W.H., Kudrolli,T.A., Yegnasubramanian,S., Luo,J., Rodriguez,R. *et al.* (2009) miR-21: an androgen receptor-regulated microRNA that promotes hormone-dependent and hormone-independent prostate cancer growth. *Cancer Res.*, **69**, 7165–7169.
36. Sun,T., Wang,Q., Balk,S., Brown,M., Lee,G.S. and Kantoff,P. (2009) The role of microRNA-221 and microRNA-222 in androgen-independent prostate cancer cell lines. *Cancer Res.*, **69**, 3356–3363.
37. Wang,X., Gocek,E., Liu,C.G. and Studzinski,G.P. (2009) MicroRNAs181 regulate the expression of p27(Kip1) in human myeloid leukemia cells induced to differentiate by 1,25-dihydroxyvitamin D(3). *Cell Cycle*, **8**, 736–741.
38. Ivanovska,I., Ball,A.S., Diaz,R.L., Magnus,J.F., Kibukawa,M., Schelter,J.M., Kobayashi,S.V., Lim,L., Burchard,J., Jackson,A.L. *et al.* (2008) MicroRNAs in the miR-106b family regulate p21/CDKN1A and promote cell cycle progression. *Mol. Cell Biol.*, **28**, 2167–2174.
39. Saramaki,A., Banwell,C.M., Campbell,M.J. and Carlberg,C. (2006) Regulation of the human p21(waf1/cip1) gene promoter via multiple binding sites for p53 and the vitamin D3 receptor. *Nucleic Acids Res.*, **34**, 543–554.
40. Bello,D., Webber,M.M., Kleinman,H.K., Wartinger,D.D. and Rhim,J.S. (1997) Androgen responsive adult human prostatic epithelial cell lines immortalized by human papillomavirus 18. *Carcinogenesis*, **18**, 1215–1223.
41. Thorne,J. and Campbell,M.J. (2008) The vitamin D receptor in cancer. *Proc. Nutr. Soc.*, **67**, 115–127.
42. VerMilyea,M.D., O'Neill,L.P. and Turner,B.M. (2009) Transcription-independent heritability of induced histone modifications in the mouse preimplantation embryo. *PLoS ONE*, **4**, e6086.
43. Velilla,E., Lopez-Bejar,M., Rodriguez-Gonzalez,E., Vidal,F. and Paramio,M.T. (2002) Effect of Hoechst 33342 staining on developmental competence of prepubertal goat oocytes. *Zygote*, **10**, 201–208.
44. Saramaki,A., Diermeier,S., Kellner,R., Laitinen,H., Vaisanen,S. and Carlberg,C. (2009) Cyclical chromatin looping and transcription factor association on the regulatory regions of the p21 (CDKN1A) gene in response to 1alpha,25-dihydroxyvitamin D3. *J. Biol. Chem.*, **284**, 8073–8082.
45. O'Neill,L.P. and Turner,B.M. (1996) Immunoprecipitation of chromatin. *Methods Enzymol.*, **274**, 189–197.
46. O'Neill,L.P., VerMilyea,M.D. and Turner,B.M. (2006) Epigenetic characterization of the early embryo with a chromatin immunoprecipitation protocol applicable to small cell populations. *Nat. Genet.*, **38**, 835–841.

47. Matilainen,M., Malinen,M., Saavalainen,K. and Carlberg,C. (2005) Regulation of multiple insulin-like growth factor binding protein genes by 1alpha,25-dihydroxyvitamin D3. *Nucleic Acids Res.*, **33**, 5521–5532.
48. Seuter,S., Vaisanen,S., Radmark,O., Carlberg,C. and Steinhilber,D. (2007) Functional characterization of vitamin D responding regions in the human 5-Lipoxygenase gene. *Biochim. Biophys. Acta.*, **1771**, 864–872.
49. Bae,V.L., Jackson-Cook,C.K., Brothman,A.R., Maygarden,S.J. and Ware,J.L. (1994) Tumorigenicity of SV40 T antigen immortalized human prostate epithelial cells: association with decreased epidermal growth factor receptor (EGFR) expression. *Int. J. Cancer*, **58**, 721–729.
50. El-Deiry,W.S., Tokino,T., Velculescu,V.E., Levy,D.B., Parsons,R., Trent,J.M., Lin,D., Mercer,W.E., Kinzler,K.W. and Vogelstein,B. (1993) WAF1, a potential mediator of p53 tumor suppression. *Cell*, **75**, 817–825.
51. Degenhardt,T., Matilainen,M., Herzig,K.H., Dunlop,T.W. and Carlberg,C. (2006) The insulin-like growth factor-binding protein 1 gene is a primary target of peroxisome proliferator-activated receptors. *J. Biol. Chem.*, **281**, 39607–39619.
52. Battaglia,S., Thorne,J., Maguire,O., Hornung,L., Sucheston,L.E., McCabe,C., Bunce,C.M. and Campbell,M.J. (2010) Elevated NCOR1 disrupts PPAR signaling in prostate cancer and forms a targetable epigenetic lesion. *Carcinogenesis*, **31**, 1501–1508.
53. O'Neill,L.P. and Turner,B.M. (2003) Immunoprecipitation of native chromatin: NChIP. *Methods*, **31**, 76–82.
54. Banwell,C.M., MacCartney,D.P., Guy,M., Miles,A.E., Uskokovic,M.R., Mansi,J., Stewart,P.M., O'Neill,L.P., Turner,B.M., Colston,K.W. *et al.* (2006) Altered nuclear receptor corepressor expression attenuates vitamin D receptor signaling in breast cancer cells. *Clin. Cancer Res.*, **12**, 2004–2013.
55. Abedin,S.A., Thorne,J.L., Battaglia,S., Maguire,O., Hornung,L.B., Doherty,A.P., Mills,I.G. and Campbell,M.J. (2009) Elevated NCOR1 disrupts a network of dietary-sensing nuclear receptors in bladder cancer cells. *Carcinogenesis*, **30**, 449–456.
56. Jensen,S.S., Madsen,M.W., Lukas,J., Binderup,L. and Bartek,J. (2001) Inhibitory effects of 1alpha,25-dihydroxyvitamin D(3) on the G(1)-S phase-controlling machinery. *Mol. Endocrinol.*, **15**, 1370–1380.
57. Campbell,M.J., Elstner,E., Holden,S., Uskokovic,M. and Koeffler,H.P. (1997) Inhibition of proliferation of prostate cancer cells by a 19-nor-hexafluoride vitamin D3 analogue involves the induction of p21waf1, p27kip1 and E-cadherin. *J. Mol. Endocrinol.*, **19**, 15–27.
58. Metivier,R., Huet,G., Gallais,R., Finot,L., Petit,F., Tiffoche,C., Merot,Y., LePeron,C., Reid,G., Penot,G. *et al.* (2008) Dynamics of estrogen receptor-mediated transcriptional activation of responsive genes in vivo: apprehending transcription in four dimensions. *Adv. Exp. Med. Biol.*, **617**, 129–138.
59. John,S., Johnson,T.A., Sung,M.H., Biddie,S.C., Trump,S., Koch-Paiz,C.A., Davis,S.R., Walker,R., Meltzer,P.S. and Hager,G.L. (2009) Kinetic complexity of the global response to glucocorticoid receptor action. *Endocrinology*, **150**, 1766–1774.
60. Ellison,T.I., Smith,M.K., Gilliam,A.C. and MacDonald,P.N. (2008) Inactivation of the vitamin D receptor enhances susceptibility of murine skin to UV-induced tumorigenesis. *J. Invest. Dermatol.*, **128**, 2508–2517.
61. Maruyama,R., Aoki,F., Toyota,M., Sasaki,Y., Akashi,H., Mita,H., Suzuki,H., Akino,K., Ohe-Toyota,M., Maruyama,Y. *et al.* (2006) Comparative genome analysis identifies the vitamin D receptor gene as a direct target of p53-mediated transcriptional activation. *Cancer Res.*, **66**, 4574–4583.
62. Lambert,J.R., Kelly,J.A., Shim,M., Huffer,W.E., Nordeen,S.K., Baek,S.J., Eling,T.E. and Lucia,M.S. (2006) Prostate derived factor in human prostate cancer cells: gene induction by vitamin D via a p53-dependent mechanism and inhibition of prostate cancer cell growth. *J. Cell Physiol.*, **208**, 566–574.
63. Kommagani,R., Caserta,T.M. and Kadakia,M.P. (2006) Identification of vitamin D receptor as a target of p63. *Oncogene*, **25**, 3745–3751.
64. Stock,J.K., Giadrossi,S., Casanova,M., Brookes,E., Vidal,M., Koseki,H., Brockdorff,N., Fisher,A.G. and Pombo,A. (2007) Ring1-mediated ubiquitination of H2A restrains poised RNA polymerase II at bivalent genes in mouse ES cells. *Nat. Cell Biol.*, **9**, 1428–1435.
65. Brookes,E. and Pombo,A. (2009) Modifications of RNA polymerase II are pivotal in regulating gene expression states. *EMBO Rep.*, **10**, 1213–1219.
66. Degenhardt,T., Rybakova,K.N., Tomaszewska,A., Mone,M.J., Westerhoff,H.V., Bruggeman,F.J. and Carlberg,C. (2009) Population-level transcription cycles derive from stochastic timing of single-cell transcription. *Cell*, **138**, 489–501.
67. Jin,F. and Fondell,J.D. (2009) A novel androgen receptor-binding element modulates Cdc6 transcription in prostate cancer cells during cell-cycle progression. *Nucleic Acids Res.*, **37**, 4826–4838.
68. Okada,M., Takezawa,S., Mezaki,Y., Yamaoka,I., Takada,I., Kitagawa,H. and Kato,S. (2008) Switching of chromatin-remodelling complexes for oestrogen receptor-alpha. *EMBO Rep.*, **9**, 563–568.
69. Cohen,E.E., Zhu,H., Lingen,M.W., Martin,L.E., Kuo,W.L., Choi,E.A., Kocherginsky,M., Parker,J.S., Chung,C.H. and Rosner,M.R. (2009) A feed-forward loop involving protein kinase Calpha and microRNAs regulates tumor cell cycle. *Cancer Res.*, **69**, 65–74.
70. Brosh,R., Shalgi,R., Liran,A., Landan,G., Korotayev,K., Nguyen,G.H., Enerly,E., Johnsen,H., Buganim,Y., Solomon,H. *et al.* (2008) p53-Repressed miRNAs are involved with E2F in a feed-forward loop promoting proliferation. *Mol. Syst. Biol.*, **4**, 229.
71. Poliseno,L., Salmena,L., Riccardi,L., Fornari,A., Song,M.S., Hobbs,R.M., Sportoletti,P., Varmeh,S., Egia,A., Fedele,G. *et al.* Identification of the miR-106b~25 microRNA cluster as a proto-oncogenic PTEN-targeting intron that cooperates with its host gene MCM7 in transformation. *Sci. Signal*, **3**, ra29.
72. Resnick,K.E., Alder,H., Hagan,J.P., Richardson,D.L., Croce,C.M. and Cohn,D.E. (2009) The detection of differentially expressed microRNAs from the serum of ovarian cancer patients using a novel real-time PCR platform. *Gynecol. Oncol.*, **112**, 55–59.
73. Mitchell,P.S., Parkin,R.K., Kroh,E.M., Fritz,B.R., Wyman,S.K., Pogosova-Agadjanyan,E.L., Peterson,A., Noteboom,J., O'Briant,K.C., Allen,A. *et al.* (2008) Circulating microRNAs as stable blood-based markers for cancer detection. *Proc. Natl Acad. Sci. USA*, **105**, 10513–10518.
74. Chen,X., Ba,Y., Ma,L., Cai,X., Yin,Y., Wang,K., Guo,J., Zhang,Y., Chen,J., Guo,X. *et al.* (2008) Characterization of microRNAs in serum: a novel class of biomarkers for diagnosis of cancer and other diseases. *Cell Res.*, **18**, 997–1006.
75. Brase,J.C., Johannes,M., Schlomm,T., Falth,M., Haese,A., Steuber,T., Beissbarth,T., Kuner,R. and Sultmann,H. Circulating miRNAs are correlated with tumor progression in prostate cancer. *Int. J. Cancer*, doi:10.1002/ijc.25376 [April 5; Epub ahead of print].